Available online at www.sciencedirect.com
ScienceDirect
European Journal of Medicinal Chemistry 44 (2009) 384–392
EUROPEAN JOURNAL OF MEDICINAL CHEMISTRY
http://www.elsevier.com/locate/ejmech

Original article

Synthesis and use of 4-peptidylhydrazido-*N*-hexyl-1,8-naphthalimides as fluorogenic histochemical substrates for dipeptidyl peptidase IV and tripeptidyl peptidase I

Ivaylo Ivanov [a], Donka Tasheva [b], Ralitza Todorova [c], Mashenka Dimitrova [c,*]

[a] *Faculty of Biology, University of Sofia ''St. Kl. Ohridsky'', 8 D. Tzankov bul, 1164 Sofia, Bulgaria*
[b] *Faculty of Chemistry, University of Sofia ''St. Kl. Ohridsky'', 1 James Bourchier Avenue, 1164 Sofia, Bulgaria*
[c] *Institute of Experimental Morphology and Anthropology with Museum, Bulgarian Academy of Sciences, Acad. G. Bonchev Street, Bl. 25, 1113 Sofia, Bulgaria*

Received 30 October 2007; received in revised form 27 February 2008; accepted 29 February 2008
Available online 18 March 2008

Abstract

Gly-Pro-, Gly-Pro-Met- and Ala-Ala-Phe-*N*′-(2-hexyl-1,3-dioxo-2,3-dihydro-1H-benzo[*de*]isoquinolin-6-yl)-hydrazides are synthesized by guanidinium/uronium type condensing reagent and used as fluorogenic substrates to localize dipeptidyl peptidase IV and tripeptidyl peptidase I activities in mammalian tissue sections. Enzyme hydrolysis releases 2-hexyl-6-hydrazino-1H-benzo[*de*]isoquinoline-1,3(2H)-dione, which couples with piperonal to form insoluble fluorescent hydrazone, precipitating on the enzyme locations and marking them. The fluorescent technique reveals precisely the enzymes locations at the lack of background noise in a single incubation step. It avoids most of the drawbacks of the previously proposed fluorescent histochemical techniques and can be valuable for the in situ studies of these enzymes in norm and pathology.

Keywords: Dipeptidyl peptidase IV; Tripeptidyl peptidase I; Fluorogenic substrates; Enzyme histochemistry; Naphthalimide derivatives

1. Introduction

Lots of peptide hydrolases are now regarded as potential markers for the diagnosis and prognosis of different malignant, immunological, inflammatory and other diseases. Amongst them, dipeptidyl peptidase IV and tripeptidyl peptidase I attract a considerable interest due to their ubiquitous distribution, multiple functions and apparent participation in the onset and progression of various diseases.

Dipeptidyl peptidase IV (DPP IV, CD26; EC 3.4.14.5) is a membrane-associated peptidase, which hydrolyzes preferentially Xaa-Pro dipeptides from free amino-terminal of three- and oligopeptides at pH optimum 7.8 [1]. It has been shown to modulate the activity of a number of biologically active substances such as pancreatic peptides, glucagon-like peptides, chemokines and endomorphins [2] and participates in the digestion of proteins, possessing proline at second position, such as collagen [3]. DPP IV has recently been named ''a moon-lighting protein'' due to the numerous functions it is found to play in the organism not only as a serine protease but also as a receptor molecule, co-stimulatory protein, adhesion molecule, etc. [4]. Aberrant DPP IV activity levels have been reported as clinically significant for various diseases as solid tumors and hematological malignancies, autoimmune, inflammatory and infectious diseases [5,6]. The enzyme is proposed as a specific diagnostic marker for thyroid carcinoma [7,8] and is regarded as a possible supporting marker for the assessment of the severity of various diseases, response to therapy and prognosis [6].

Tripeptidyl peptidase I (TPP I, EC 3.4.14.9) is a lysosomal serine protease, cleaving off tripeptides from oligo- and polypeptides at acid pH optimum of 4.5 [9]. The rat enzyme is specific towards substrates, possessing Gly-Pro-Met or Ala-Ala-Phe tripeptide at the N-terminal [10], whereas Ala-Ala-Phe amino

* Corresponding author. Tel.: +359 2 979 23 07; fax: +359 2 719007.
E-mail address: mashadim@abv.bg (M. Dimitrova).

0223-5234/$ - see front matter © 2008 Elsevier Masson SAS. All rights reserved.
doi:10.1016/j.ejmech.2008.02.036

acid sequence is the most favourable for the human TPP I [11]. Natural substrates of TPP I are not clearly established, but it has been reported that the enzyme participates in the hydrolysis of collagen [11] and peptide hormones like glucagons, angiotensines II and III [10], substance P [12] and neuromedine B [13]. Mutations in the gene CLN2, which encodes TPP I cause the late infantile neuronal ceroid lipofuscinosis (LINCL) – a fatal neurodegenerative disease with a typical onset at the age of 2–4. It is characterized by mental regression, seizures, visual loss and fetal end usually at puberty [14]. Some mutations in CLN2 can cause atypical phenotypes, demonstrated by a delayed onset and slower progression of the symptoms [15]. The diagnosis of LINCL and its discrimination from the other forms of neuronal ceroid lipofuscinosis (NCL) relies on the determination of TPP I activity level and a subsequent confirmation by DNA mutation analysis [16]. TPP I is over-expressed in various pathological conditions, i.e. malignant, neurodegenerative and inflammatory diseases and is proposed as a marker enzyme for the breast cancer [12].

DPP IV and TPP I hydrolyze synthetic substrates and their activities are usually studied using *para*-nitroanilide or methylcoumarylamide substrates. Histochemical studies of DPP IV are performed either by chromogenic substrates or by immunohistochemistry, whereas TPP I is visualized in situ exclusively by immunohistochemical methods [17,18]. Fluorogenic substrates for the two enzymes are not accepted for routine use, though different attempts to develop such substrates have been done in our laboratory as well [19,20]. Both enzymes are shown to cleave off hydrazide bond of synthetic substrates [19–22]. A promising possibility in this respect represents the 4-hydrazino-*N*-alkyl-1,8-naphthalimide derivatives, the properties of which have been studied by Gan et al. [23]. The authors show that these compounds have weak green fluorescence in solid state ($\lambda_{em} = 540$ nm), but their hydrazones with aromatic aldehydes, possessing electron-donating groups at *para*-position demonstrate a large batochromic shift in the fluorescent spectra ($\lambda_{em} > 640$ nm) and a subsequent increase in the fluorescence intensity. These properties have been used to obtain highly fluorescent ferocene complexes [24].

In the present paper we describe the synthesis of specific fluorogenic substrates, based on 4-hydrazino-*N*-hexyl-1,8-naphthalimide (HHNI) for DPP IV (Gly-Pro–HHNI) and TPP I (Gly-Pro-Met–HHNI and Ala-Ala-Phe–HHNI) and the development of novel fluorescent techniques for the histochemical visualization of these enzymes. The newly synthesized substrates are applied successfully for the localization of the two enzymes in tissue sections from rat and mouse organs. The herein-developed techniques can be used in future studies in normal and pathologically altered tissues and may be a useful tool for the diagnosis and prognosis of diseases, for which DPP IV and TPP I are marker enzymes.

2. Molecular modeling

According to the crystal structure of human DPP IV, obtained by Thoma et al. [25], substrates with different leaving groups may bind the enzyme active centre through the widely open active site cleft. It has been shown [19–22], that DPP IV can hydrolyze dipeptidyl hydrazide derivatives of 9,10-anthraquinone. However, the substrates, based on 4-hydrazino-*N*-alkyl-1,8-naphthalimide have a leaving group of different structures. Using the crystal structure of human DPP IV complex with Diprotin A (entry number 1nu8), we modeled the structure of the enzyme–substrate complex with Gly-Pro–HHNI by Dreiding force field method [26]. The molecular model of the complex shows, that O^{γ} atom of Ser630 is at a distance of 3.0 Å from the carbonyl carbon of proline and is favourably disposed for a nucleophilic attack. The carbonyl oxygen of proline forms a hydrogen bond with O^{η} atom of Tyr547 (2.7 Å) and N^{α} atom of Tyr631 (3.2 Å), which shape the oxyanion hole. The substrate nitrogen bound to the carbonyl group of proline is at a distance of 3.5 Å from $N^{\varepsilon 2}$ atom of His740. The naphthalimide moiety and the alkyl chain participate only in hydrophobic interactions with the amino acid residues of the enzyme active site. The most favourable length of the alkyl chain is six to eight carbon atoms (Supplementary data, Fig. 4).

3. Chemistry

4-Hydrazino-*N*-hexyl-1,8-naphthalimide (HHNI, **1**) was prepared from 4-chloro-*N*-hexyl-1,8-naphthalimide and hydrazine hydrate by the procedure described by Zhu et al. [27] with modifications. First attempts to couple HHNI (**1**) to Boc-amino acid were conducted through carbodiimide method in the presence of 1-hydroxybenzotriazole [21], but this procedure gave very low yields of the respective hydrazides. The main product was identified (TLC) as the compound formed by carbodiimide and HHNI in the absence of *N*-protected amino acid under the same reaction conditions. Most probably, the carbodiimides react preferentially with **1**, thus preventing the formation of the desired hydrazide. The *N*-protected aminoacyl hydrazides were obtained in much higher yields by applying the standard protocol with TBTU as coupling reagent (Scheme 1). As a first step, the activation of the acyl component was performed by its conversion to benzotriazole active ester using TBTU and subsequently HHNI is added to the reaction mixture. In the case of Boc-Gly-Pro-OH (**2**), the activation step was carried out at −15 °C in order to suppress the racemization. The same procedure was applied during the synthesis of tripeptide derivatives (**8**,**9**) from the corresponding *N*-protected dipeptides and aminoacyl hydrazides (Scheme 1). The substrates for DPP IV and TPP I were obtained by cleaving off the protective groups from the respective Boc- or Z-peptidyl hydrazides.

4. Histochemical results and discussion

The fluorescent histochemical principle presented here for the visualization of DPP IV and TPP I activity locations is illustrated in Scheme 2. The enzyme hydrolyzes the corresponding synthetic substrate to yield free HHNI, which couples simultaneously with an aromatic aldehyde and gives a water-insoluble fluorescent hydrazone, precipitating on the sites of enzyme activity. Different aldehydes possessing

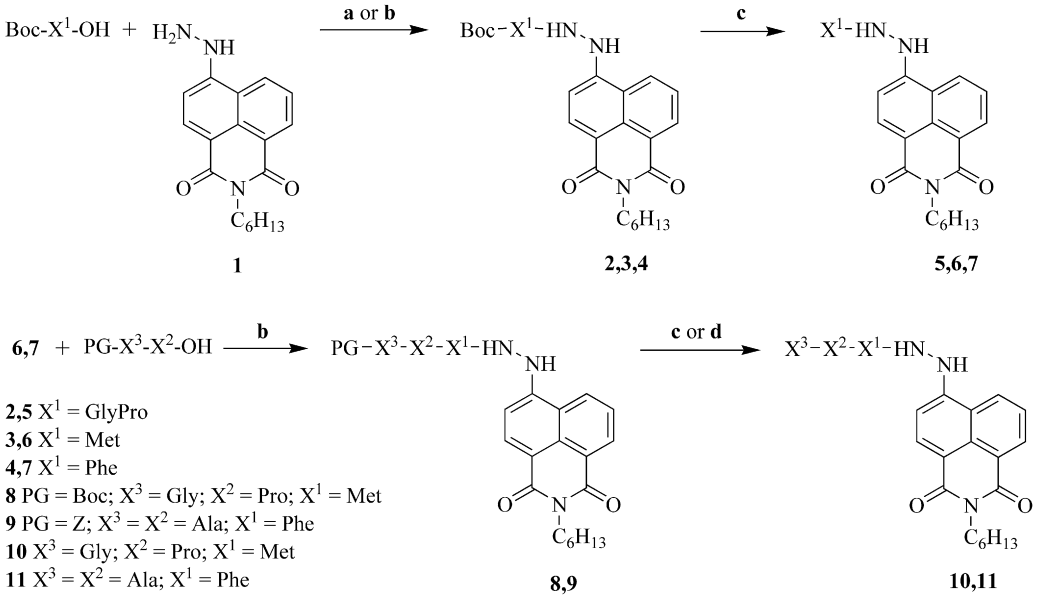

Scheme 1. Reagents and conditions: (a) TBTU, HOBt, DIPEA (3 eq) in DMF, 1 h, rt; (b) TBTU, HOBt, DIPEA (2 eq) in DMF, 1 h, −15 °C and 1 h, rt; (c) 4 M HCl/dioxane; (d) 5.7 M HBr/acetic acid.

electron-donating substituents (di- or three-substituted benzaldehydes with hydroxy and/or alkoxy groups) or electron-withdrawing substituents (4-substituted benzaldehydes with nitro, cyano and aldehyde groups) were tested. Those with electron-withdrawing substituents gave rough crystalline hydrazones practically not fluorescing over 590 nm on tissue sections. The aldehydes with electron-donating groups had hydrazones of microcrystalline to amorphous appearance and brilliant red fluorescence on the sections. Best results were obtained with piperonal – its hydrazone is amorphous and has a strong fluorescence over 600 nm – both in solid state and in solution (Fig. 1). The enzyme reaction can be observed either by light microscopy where the final reaction product is visible as red precipitates or by fluorescent microscopy at minimal or none fluorescent background noise (Figs. 2 and 3). The application of this principle for DPP IV localization is shown in Fig. 2. It demonstrates the characteristic enzyme sites in epididymis, small intestine, spleen and liver. The specificity of the enzyme reaction was confirmed by inhibition studies using the irreversible DPP IV inhibitor Phe-Pro–NHONb to show a weak residual activity only in the small intestinal enterocytes, indicated by single fluorescent dots (Fig. 2c1, d1). Fig. 3 shows TPP I activity distribution in several rat and mouse organs, obtained by the novel fluorescent technique. The final reaction product was deposited within the cells in the form of small granules corresponding to the lysosomal localization of the enzyme. Using Gly-Pro-Met–HHNI as substrate, 3 h of incubation was enough to visualize the enzyme sites in all the organs studied, whereas the other substrate – Ala-Ala-Phe–HHNI required twice longer incubation period. Incubation of control sections in the presence of TPP I specific inhibitor Ala-Ala-Phe–chloromethyl ketone totally abolished the enzyme activity confirming that the substrates were not hydrolyzed by other peptidases at the low pH optimum of this enzyme.

We have previously proposed a fluorescent histochemical technique for the visualization of DPP IV and TPP I using substrates, based on 2-anthraquinonylhydrazine and 3-nitrobenzaldehyde as a coupling reagent [19,20]. This technique proved successful for the localization of the two enzymes in different rat organs. Obviously, it was founded on a similar principle as the procedure presented here, i.e. enzyme hydrolysis of the substrate, followed by a coupling step with an

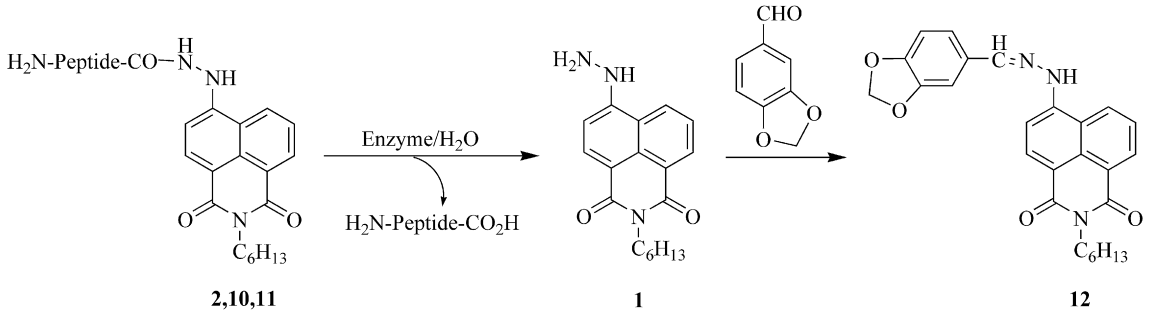

Scheme 2. Principle for detection of DPP IV and TPP I activity.

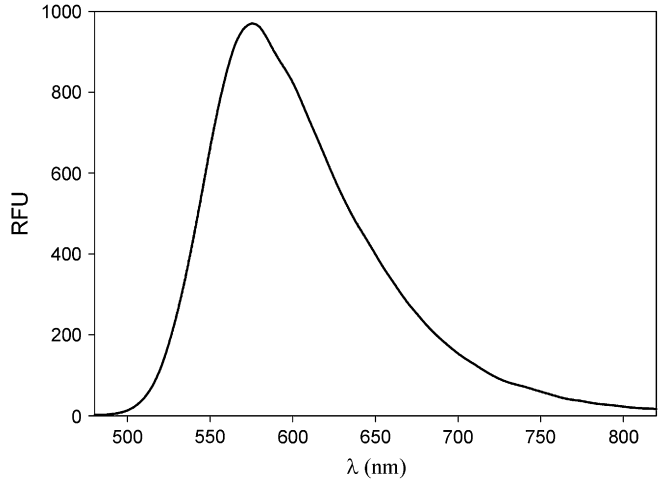

Fig. 1. Fluorescent spectrum of 6-{*N*′-[1-benzo[1,3]dioxol-5-yl-methylidene]-hydrazino}-2-hexyl-benzo[*de*]isoquinoline-1,3-dione (**12**) in dimethyl sulfoxide (λ_{ex} 460 nm).

aromatic aldehyde to obtain a fluorescent insoluble hydrazone. A significant distinction between the two methods, however, represents the use of different aldehydes. The first method employs a highly reactive benzaldehyde with an electron-withdrawing group (nitro group). It binds to a great extent to the free amino group of the substrate, thus decreasing the substrate accessibility in the incubation medium. This flaw is overcome in the present method by using a benzaldehyde with electron-donating substituents. Another difference between the two procedures is the duration of the visualization process. The former procedure included a post-coupling step of additional incubation of the sections in buffered aldehyde, whereas the novel one allows the enzyme activity visualization in a single step. Taking into account the fact that the synthetic pathway of 2-anthraquinonyl hydrazides includes the use of a cancerogenic substance (2-aminoanthraquinone), the presented novel fluorescent histochemical procedure can be considered much improved.

5. Conclusions

We have designed, synthesized and tested a new type of fluorogenic substrates, intended for the in situ visualization of DPP IV and TPP I by their activities. Using these substrates, we have developed fluorescent histochemical procedures, derived from the ability of both enzymes to hydrolyze hydrazide bond and the considerable differences in fluorescence spectra of 4-hydrazino-*N*-hexyl-1,8-naphthalimide and its hydrazones with aromatic aldehydes, possessing electron-donating substituents in the aromatic ring. Application of these techniques in tissue sections of rat and mouse organs revealed precisely the locations of DPP IV and TPP I activities at the lack of background fluorescence noise after a single incubation step of a reasonable duration. The here-proposed procedures might open new possibilities in the in situ studies of the enzymes activities and might serve as valuable tools for the diagnosis, response to therapy and prognosis of the diseases, for which they are marker enzymes.

6. Experimental protocols

6.1. General

Initial graphic visualization and manipulation of molecules were performed using the program DS VIEWERPRO 6.0 (Accelrys Corporation, San Diego, CA, USA; http://www.accelrys.com/dstudio/ds_viewer/index.html). Models were based on the crystallographic coordinates of the crystal structure of human DPP IV complex with Diprotin A (Ile-Pro-Ile), Brookhaven Protein Data Bank (pdb code: 1nu8).

^{1}H NMR spectra were obtained using a Bruker Avance AV II+ 600 MHz NMR spectrometer using tetramethyl silane as an internal standard. Chemical shifts (δ) are expressed in parts per million and coupling constants (J) in hertz. Elemental analyses were performed by VarioEL V5, CHNS Mode, Elementar Analysensysteme GmbH. Microanalyses (C, H, N) of new compounds agreed with the theoretical value within ±0.4%. Measurements of fluorescence spectra were performed on Varioscan® ThermoElectron, USA. Absorption spectra were made on UV/visible spectrophotometer Ultrospec 3000, Pharmacia Biotech. Melting points were determined on a Botius micro melting point apparatus and were uncorrected.

Tissue sections were cut on cryotome Reichert-Jung, model 2800 (Nussloch, FRG). Enzyme reactions were observed under microscope OPTON IM 35 (FRG). Microphotographs were made on Konika Minolta 200 ASA colourful films.

4-Chloro-1,8-naphthalic anhydride, hydrazine monohydrate, dimethyl sulfoxide (DMSO), *N*-[(1H-benzotriazol-1-yl) (dimethylamino)methylene]-*N*-methylmethanaminium tetrafluoroborate *N*-oxide (TBTU), 4 M HCl/dioxane, 5.7 M HBr/acetic acid, diethylether, hexylamine, isopropanol, celloidin, gummy arabic, *N*,*N*-dimethyl formamide (DMF) and silica gel 60 (0.063–0.200 mm) were purchased from Fluka. 1-Hydroxybenzotriazole (HOBt), Boc-Gly-Pro-OH, Boc-Met-OH, Boc-Phe-OH, Z-Ala-Ala-OH and TPP I inhibitor – H-Ala-Ala-Phe–chloromethylketone were from Bachem AG. Absolute ethanol was from Riedel de Haen, *N*,*N*-diisopropylethylamine (DIPEA) and piperonal – from Sigma–Aldrich, hexane and acetone – from Lab-Scan. The DPP IV inhibitor – *N*-(H-Phe-Pro-)-O-(4-nitrobenzoyl)hydroxylamine hydrochloride (Phe-Pro-NHONb) was synthesized according to Ref. [28].

6.2. Molecular modeling

The structures of enzyme–substrate complexes with docked substrates were refined by the following procedure. First, the N-terminal isoleucine was transformed into glycine by removing the side chain. Then, chemical bond between O^{γ} atom of Ser630 and proline moiety of the substrate was also removed and the carbonyl group was restored. The C-terminal isoleucine was replaced by 4-hydrazino-*N*-alkyl-1,8-naphthalimide. Finally all the atoms of the enzyme were fixed except for those of the side chain of the catalytic Ser630. Their positions together with the coordinates of the substrate atoms were optimized using the Dreiding force field.

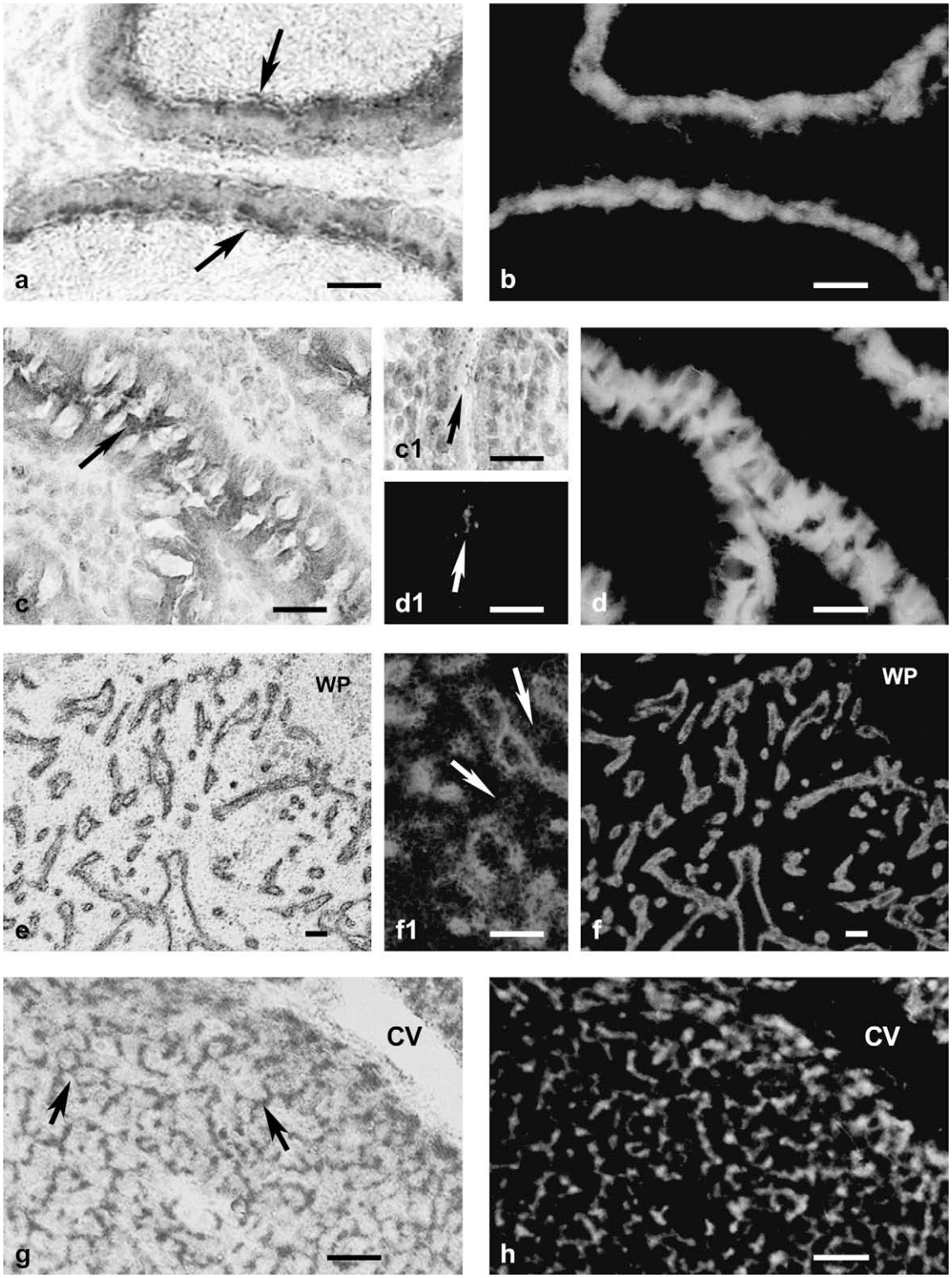

Fig. 2. Histochemical demonstration of DPP IV activity in rat and mouse organs with the substrate Gly-Pro–HHNI and piperonal as a coupling agent. (a), (b) – rat epididymis: enzyme reaction in duct epithelial cells particularly strong in the stereocilia (arrows), originally × 400; (c), (d) – rat jejunum: final reaction product in the enterocytes most abundant in the brush border area (arrow), originally × 400; (c1), (d1) – inhibitor experiment in the small intestine: residual DPP IV activity represented as isolated fluorescent dots in the brush borders of the enterocytes (arrows), originally × 400; (e), (f) – rat spleen: DPPIV activity in sinusoids and veins of the red pulp (WP – white pulp), originally × 200; (f1) – part of the rat spleen red pulp: fluorescence microscopy allows to see that lymphocytes, surrounding blood vessels are also DPP IV positive (arrows), originally × 400; (g), (h) – mouse liver: enzyme reaction in hepatocytes especially strong in the cell periphery (arrows) (CV – central vein), originally × 400. (a), (c), (c1), (e), (g) – light microscopy; (b), (d), (d1), (f), (f1), (h) – fluorescence microscopy; scale bar = 20 μm.

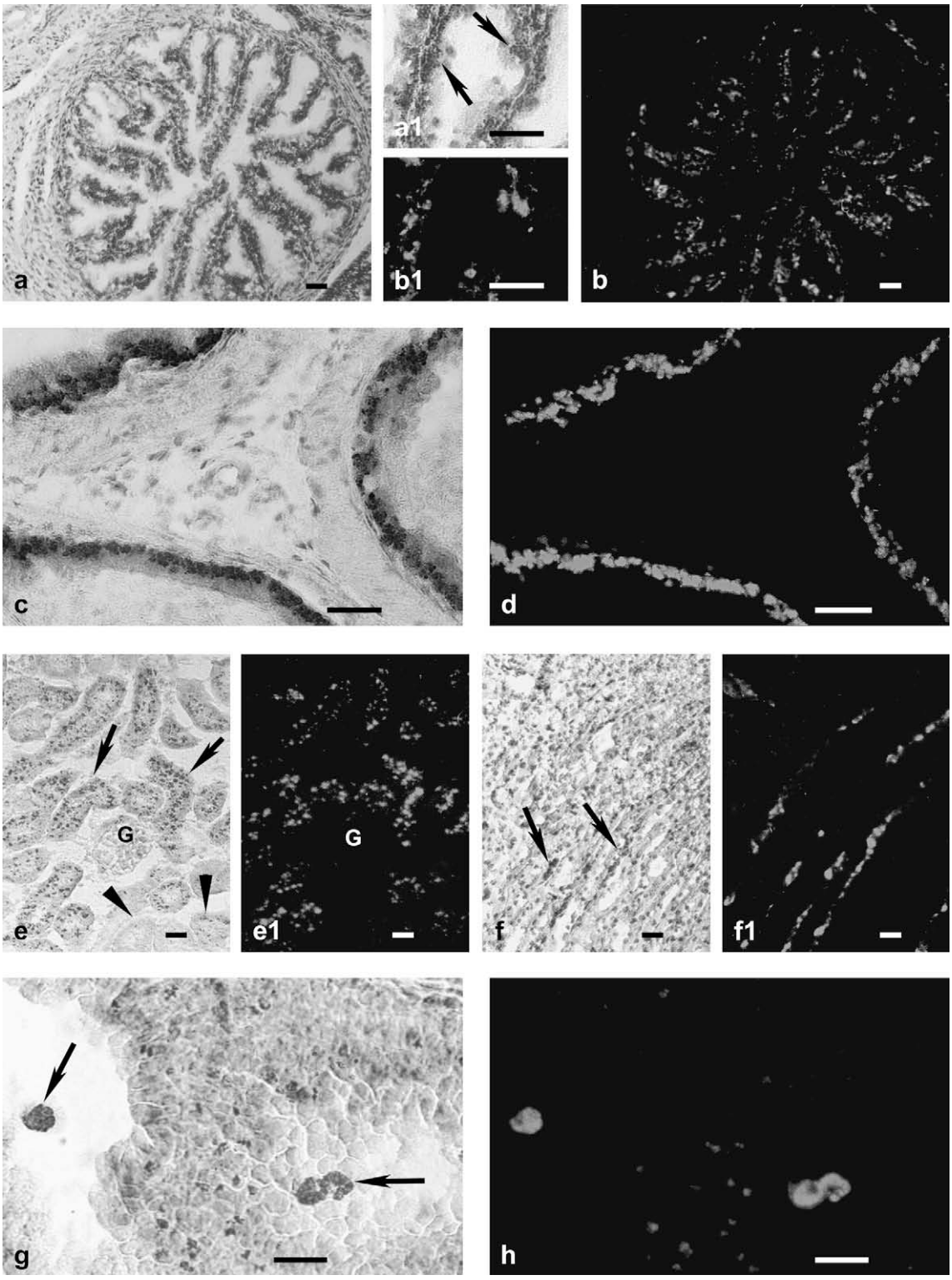

Fig. 3. Histochemical localization of TPP I activity in rat and mouse organs with the substrate Gly-Pro-Met–HHNI and piperonal. (a), (b) – mouse fallopian tube: TPP I activity in the epithelial cells of the mucosal folds, originally × 200; (a1), (b1) – mucosal folds: final reaction product is localized intra-cellularly in the form of red granules, originally × 400; (c), (d) – rat epididymis: high enzyme reaction in the epithelial cells of the channels, originally × 400; (e), (e1) – rat kidney cortex: fine granular reaction, high (arrows) or low to none (arrowheads) in the epithelial cells of the convoluted tubules, no reaction product in the glomeruli (G), originally × 200: (f), (f1) – rat kidney medulla: some of the straight tubules are TPP I positive (arrows), originally × 200; (g), (h) – rat lung: intense reaction of TPP I in the macrophages (arrows) and weak in the bronchial epithelium, originally × 600. (a), (a1), (c), (e), (f), (g) – light microscopy; (b), (b1), (d), (e1), (f1), (h) – fluorescence microscopy; scale bar = 20 μm.

6.3. Chemistry

6.3.1. Synthesis of 6-chloro-2-hexyl-1H-benzo[de]isoquinoline-1,3(2H)-dione

This was performed following the procedure described in Ref. [29]. In brief, 0.66 g (2.84 mmol) 4-chloro-1,8-naphthalic anhydride and 0.38 ml (2.84 mmol) hexylamine were boiled in 30 ml absolute ethanol until the anhydride dissolved completely (10–12 h). The clear yellow solution was allowed to precipitate at room temperature and the obtained precipitate was gathered by filtration. Then, it was recrystallized from isopropanol to obtain yellowish-white crystals. Yield 0.48 g (54%); m.p. 71–73 °C.

6.3.2. Synthesis of 2-hexyl-6-hydrazino-1H-benzo[de]isoquinoline-1,3(2H)-dione (**1**)

6-Chloro-2-hexyl-benzo[*de*]isoquinoline-1,3-dione (1.07 g, 3.4 mmol) and hydrazine hydrate (0.5 ml, 10.2 mmol) were dissolved in 7 ml DMSO and stirred under N_2 at 60 °C for 4 h. The reaction mixture was poured into 8% aqueous sulfuric acid. The yellow precipitate was filtered and recrystallized from ethanol. Yield 0.45 g (43%); m.p. 177–180 °C; UV–vis (ethanol): λ_{max} 445 nm.

The compound was used for synthesis without further purification.

6.3.3. General procedure for acylation of **1**

N-tert-Butoxycarbonyl amino acid (1 mmol), TBTU (0.32 g, 1 mmol), HOBt hydrate (0.16 g, 1 mmol) and DIPEA (0.52 ml, 3 mmol) in 3 ml DMF were mixed for 5 min at room temperature, after which **1** (0.31 g, 1 mmol) was added. The reaction mixture was stirred at room temperature for an hour, poured into 5% $NaHCO_3$ and the precipitate was collected by filtration, dried in vacuum over $CaCl_2$ and purified by column chromatography on silica gel.

Boc-Gly-Pro-OH was coupled to **1** in the same manner, but the reaction was carried out at −15 °C for an hour and one more hour at room temperature.

6.3.3.1. N-tert-Butoxycarbonyl-glycyl-L-proline N′-(2-hexyl-1,3-dioxo-2,3-dihydro-1H-benzo[de]isoquinolin-6-yl)hydrazide (**2**).

Chromatography: hexane/acetone 2:1; yield 0.33 g (59%). ^{1}H NMR (DMSO-d_6) δ ppm: 10.27 (s, 1H, NHN*H*CO), 9.61 (s, 1H, NHN*H*Ar), 8.70 (d, 1H, $J = 8.4$ Hz, Ar), 8.47 (d, 1H, $J = 7.2$ Hz, Ar), 8.29 (d, 1H, $J = 8.4$ Hz, Ar), 7.75 (t, 1H, $J = 7.9$ Hz, Ar), 7.02 (d, 1H, $J = 8.4$ Hz, Ar), 6.92 (t, 1H, $J = 5.8$ Hz, OCON*H*), 4.46 (dd, 1H, $J = 8.6$, 3.2 Hz, α-Pro), 4.01 (t, 2H, $J = 7.5$, NCH_2), 3.83 (d, 2H, $J = 5.8$, α-Gly), 3.65–3.61 (m, 1H, δ-Pro), 3.55–3.51 (m, 1H, δ-Pro), 2.22–2.17 (m, 1H, β-Pro), 2.02–1.95 (m, 3H, β-Pro, γ-Pro), 1.63–1.58 (m, 2H, NCH_2CH_2), 1.41 (s, 9H, $COOC(CH_3)_3$), 1.35–1.28 (m, 6H, $NCH_2CH_2(CH_2)_3CH_3$), 0.86 (t, 3H, $J = 6.9$ Hz, $N(CH_2)_5CH_3$); UV–vis (ethanol): λ_{max} 415 nm.

6.3.3.2. N-tert-Butoxycarbonyl-L-methionine N′-(2-hexyl-1,3-dioxo-2,3-dihydro-1H-benzo[de]isoquinolin-6-yl)hydrazide (**3**).

Chromatography: hexane/acetone 3.5:1; yield 0.44 g (81%). ^{1}H NMR (DMSO-d_6) δ ppm: 10.38 (s, 1H, NHN*H*CO), 9.62 (s, 1H, NHN*H*Ar), 8.69 (d, 1H, $J = 7.2$, Ar), 8.48 (d, 1H, $J = 7.2$ Hz, Ar), 8.23 (d, 1H, $J = 8.4$ Hz, Ar), 7.76 (t, 1H, $J = 7.9$ Hz, Ar), 7.33 (d, 1H, $J = 7.5$ Hz, OCONH), 6.99 (d, 1H, $J = 8.4$ Hz, Ar), 4.21–4.17 (m, 1H, α-Met), 4.01 (t, 2H, $J = 7.4$ Hz, NCH_2), 2.32–2.29 (m, 2H, γ-Met), 2.10 (s, 3H, SCH_3), 1.98–1.94 (m, 2H, β-Met), 1.62–1.59 (m, 2H, NCH_2CH_2), 1.45 (s, 9H, $COOC(CH_3)_3$), 1.32–1.24 (m, 6H, $NCH_2CH_2(CH_2)_3CH_3$), 0.86 (t, 3H, $J = 6.9$ Hz, $N(CH_2)_5CH_3$); UV–vis (ethanol): λ_{max} 415 nm.

6.3.3.3. N-tert-Butoxycarbonyl-L-phenylalanine N′-(2-hexyl-1,3-dioxo-2,3-dihydro-1H-benzo[de]isoquinolin-6-yl)hydrazide (**4**).

Chromatography: hexane/acetone 3.5:1; yield 0.42 g (75%). ^{1}H NMR (DMSO-d_6) δ ppm: 10.42 (s, 1H, NHN*H*CO), 9.64 (s, 1H, NHN*H*Ar), 8.71 (d, 1H, $J = 8.5$ Hz, Ar), 8.48 (d, 1H, $J = 7.3$ Hz, Ar), 8.14 (d, 1H, $J = 8.4$ Hz, Ar), 7.75 (t, 1H, $J = 7.8$ Hz, Ar), 7.40–7.32 (m, 5H, Ph), 7.31–7.27 (m, 1H, OCON*H*), 6.62 (d, 1H, $J = 8.4$ Hz, Ar), 4.41–4.36 (m, 1H, α-Phe), 4.01 (t, 2H, $J = 7.5$ Hz, NCH_2), 3.06 (dd, 1H, $J = 13.6$, 5.7 Hz, β-Phe), 2.94 (dd, 1H, $J = 13.4$, 9.6 Hz, β-Phe), 1.64–1.57 (m, 2H, NCH_2CH_2), 1.39 (s, 9H, $COOC(CH_3)_3$), 1.34–1.25 (m, 6H, $NCH_2CH_2(CH_2)_3CH_3$), 0.86 (t, 3H, $J = 6.8$ Hz, $N(CH_2)_5CH_3$); UV–vis (ethanol): λ_{max} 415 nm.

6.3.4. General procedure to remove Boc-protecting group

The protected compound (0.5 mmol) was stirred in 2.5 ml 4 M HCl/dioxane for an hour at room temperature. Diethyl ether was added dropwise until the yellow product separated. Then it was collected by filtration.

6.3.4.1. Glycyl-L-proline N′-(2-hexyl-1,3-dioxo-2,3-dihydro-1H-benzo[de]isoquinolin-6-yl)-hydrazide, hydrochloride (Gly-Pro–HHNI, **5**).

Recrystallized from ethanol/diethyl ether; yield 0.24 g (94%). ^{1}H NMR (DMSO-d_6) δ ppm: 10.46 (s, 1H, NHN*H*CO), 9.69 (s, 1H, NHN*H*Ar), 8.69 (d, 1H, $J = 8.5$ Hz, Ar), 8.48 (d, 1H, $J = 7.2$ Hz, Ar), 8.13 (d, 1H, $J = 8.5$ Hz, Ar), 8.04 (br s, 3H, NH_3^+), 7.75 (t, 1H, $J = 7.9$ Hz, Ar), 6.41 (d, 1H, $J = 8.5$ Hz, Ar), 4.77–4.72 (m, 1H, α-Pro), 4.46–4.42 (m, 1H, α-Gly), 4.01 (t, 2H, $J = 7.4$ Hz, NCH_2), 3.89–3.83 (m, 1H, α-Gly), 3.11 (dd, 1H, $J = 13.6$, 6.8 Hz, δ-Pro), 2.99 (dd, 1H, $J = 13.6$, 8.4 Hz, δ-Pro), 1.62–1.58 (m, 2H, NCH_2CH_2), 1.33–1.28 (m, 8H, $NCH_2CH_2(CH_2)_3CH_3$, β-Pro), 1.26–1.24 (m, 2H, γ-Pro), 0.86 (t, 3H, $J = 6.8$ Hz, $N(CH_2)_5CH_3$).

6.3.5. Synthesis of **8** and **9**

Boc-Gly-L-Pro-OH (0.11 g, 0.4 mmol) or Z-L-Ala-L-Ala-OH (0.12, 0.4 mmol), TBTU (0.13 g, 0.4 mmol) and HOBt hydrate (0.06 g, 0.4 mmol) in DMF (1.2 ml) were mixed and allowed to cool to −15 °C (ice-salt bath). After that DIPEA (0.14 ml, 0.8 mmol) was added and the mixture was stirred for 5 min. Then, 0.4 mmol of the corresponding deprotected amino acid hydrazide (**6** or **7**) and DIPEA (0.07 ml, 0.4 mmol) were added. The reaction mixture was stirred at −15 °C for an hour and at room temperature for an additional

hour and then treated according to the general procedure in Section 6.3.3.

*6.3.5.1. N-tert-Butoxycarbonyl-glycyl-L-prolyl-L-methionine N′-(2-hexyl-1,3-dioxo-2,3-dihydro-1H-benzo[de]isoquinolin-6-yl)-hydrazide (**8**).* Chromatography: hexane/acetone 1:1.3; yield 0.2 g (72%). ^{1}H NMR (DMSO-d_6) δ ppm: 10.23 (s, 1H, NHN*H*CO), 9.63 (s, 1H, NHN*H*Ar), 8.69 (d, 1H, $J = 8.4$ Hz, Ar), 8.48 (d, 1H, $J = 7.3$ Hz, Ar), 8.33 (d, 1H, $J = 7.8$ Hz, CON*H*), 8.27 (d, 1H, $J = 8.4$ Hz, Ar), 7.76 (t, 1H, $J = 7.9$ Hz, Ar), 6.90 (d, 1H, $J = 8.4$ Hz, Ar), 6.71 (t, 1H, $J = 5.7$ Hz, OCON*H*), 4.52–4.48 (m, 1H, α-Met), 4.39 (dd, 1H, $J = 8.2$, 3.3 Hz, α-Pro), 4.01 (t, 2H, $J = 7.4$ Hz, NCH_2), 3.82 (dd, 1H, $J = 16.9$, 5.8 Hz, α-Gly), 3.77 (dd, 1H, $J = 16.9$, 5.6 Hz, α-Gly), 3.60–3.57 (m, 1H, δ-Pro), 3.50–3.47 (m, 1H, δ-Pro), 2.65–2.60 (m, 1H, γ-Met), 2.55–2.52 (m, 1H, γ-Met), 2.11 (s, 3H, SCH_3), 2.07–2.04 (m, 2H, β-Pro), 1.99–1.96 (m, 2H, β-Met), 1.94–1.90 (m, 1H, γ-Pro), 1.87–1.85 (m, 1H, γ-Pro), 1.62–1.58 (m, 2H, NCH$_2$CH_2), 1.34 (s, 9H, COOC(CH_3)$_3$), 1.33–1.28 (m, 6H, NCH$_2$CH$_2$(CH_2)$_3$CH$_3$), 0.86 (t, 3H, $J = 6.9$ Hz, N(CH$_2$)$_5$CH_3); UV–vis (ethanol): λ_{max} 415 nm.

*6.3.5.2. N-Benzyloxycarbonyl-L-alanyl-L-alanyl-L-phenylalanine N′-(2-hexyl-1,3-dioxo-2,3-dihydro-1H-benzo[de]isoquinolin-6-yl)-hydrazide (**9**).* Recrystallized from acetonitrile; yield 0.24 g (82%). ^{1}H NMR (DMSO-d_6) δ ppm: 10.36 (s, 1H, NHN*H*CO), 9.62 (s, 1H, NHN*H*Ar), 8.69 (d, 1H, $J = 8.5$ Hz, Ar), 8.47 (d, 1H, $J = 7.3$ Hz, Ar), 8.33 (d, 1H, $J = 8.0$ Hz, CON*H*), 8.11 (d, 1H, $J = 8.4$ Hz, Ar), 8.00 (d, 1H, $J = 7.4$ Hz, CON*H*), 7.74 (t, 1H, $J = 7.8$ Hz, Ar), 7.49 (d, 1H, $J = 7.3$ Hz, OCON*H*), 7.38–7.31 (complex m, 10H, Ph), 6.35 (d, 1H, $J = 8.4$ Hz, Ar), 5.06–5.00 (m, 2H, CH_2OCO), 4.75–4.71 (m, 1H, α-Phe), 4.34–4.32 (m, 1H, α-Ala), 4.09–4.04 (m, 1H, α-Ala), 4.00 (t, 2H, $J = 7.5$ Hz, NCH_2), 3.12–3.09 (m, 1H, β-Phe), 3.02–2.98 (m,1H, β-Phe), 1.62–1.58 (m, 2H, NCH$_2$CH_2), 1.34–1.28 (m, 6H, NCH$_2$CH$_2$(CH_2)$_3$CH$_3$), 1.21 (d, 3H, $J = 7.5$ Hz, β-Ala), 1.19 (d, 3H, $J = 7.4$ Hz, β-Ala), 0.86 (t, 3H, $J = 6.7$ Hz, N(CH$_2$)$_5$CH_3); UV–vis (ethanol): λ_{max} 415 nm.

*6.3.6. Preparation of glycyl-L-prolyl-L-methionine N′-(2-hexyl-1,3-dioxo-2,3-dihydro-1H-benzo[de]isoquinolin-6-yl)-hydrazide, hydrochloride (**10**)*

Compound **10** was obtained from **8** following the procedure described in Section 6.3.4. Yield 0.28 g (87%). ^{1}H NMR (DMSO-d_6) δ ppm: 10.40 (s, 1H, NHN*H*CO), 9.66 (s, 1H, N*H*NHAr), 8.70 (d, 1H, $J = 8.5$ Hz, Ar), 8.53 (d, 1H $J = 7.8$ Hz, CON*H*), 8.49 (d, 1H, $J = 7.2$ Hz, Ar), 8.26 (d, 1H, $J = 8.4$ Hz, Ar), 8.16 (br s, 3H, NH_3^+), 7.77 (t, 1H, $J = 7.9$ Hz, Ar), 6.90 (d, 1H, $J = 8.4$ Hz, Ar), 4.53–4.50 (m, 1H, α-Met), 4.46 (dd, 1H, $J = 8.4$, 3.3 Hz, α-Pro), 4.01 (t, 2H, $J = 7.4$ Hz, NCH_2), 3.89–3.81 (m, 2H, α-Gly), 3.65–3.61 (m, 1H, δ-Pro), 3.53–3.49 (m, 1H, δ-Pro), 2.66–2.62 (m, 1H, γ-Met), 2.55–2.52 (m, 1H, γ-Met), 2.13 (s, 3H, SCH_3), 2.09–2.05 (m, 2H, β-Pro), 2.02–1.97 (m, 2H, β-Met), 1.94–1.89 (m, 2H, γ-Pro), β-Met 1.62–1.58 (m, 2H, NCH$_2$CH_2), 1.34–1.28 (m, 6H, NCH$_2$(CH_2)$_3$CH$_3$), 0.86 (t, 3H, $J = 6.8$ Hz, N(CH$_2$)$_5$CH_3).

*6.3.7. Preparation of L-alanyl-L-alanyl-L-phenylalanine N′-(2-hexyl-1,3-dioxo-2,3-dihydro-1H-benzo[de]isoquinolin-6-yl)-hydrazide, hydrobromide (**11**)*

Compound **9** (0.37 g, 0.5 mmol) was treated with 1 ml 5.7 M HBr/acetic acid for 20 min at room temperature. Diethyl ether was added dropwise and the separated solid product was filtered, washed with diethyl ether and recrystallized from ethanol/diethyl ether. Yield 0.28 g (82%). ^{1}H NMR (DMSO-d_6) δ ppm: 10.46 (s, 1H, NHN*H*CO), 9.63 (s, 1H, NHN*H*Ar), 8.69 (d, 1H, $J = 8.5$ Hz, Ar), 8.55 (d, 1H, $J = 7.8$ Hz, CON*H*), 8.53 (d, 1H, $J = 8.2$ Hz, CON*H*), 8.48 (d, 1H, $J = 7.2$ Hz, Ar), 8.13 (d, 1H, $J = 8.5$ Hz, Ar), 8.04 (br s, 3H, NH_3^+), 7.75 (t, 1H, $J = 7.9$ Hz, Ar), 7.39–7.31 (m, 5H, Ph), 6.41 (d, 1H, $J = 8.4$ Hz, Ar), 4.76–4.72 (m, 1H, α-Phe), 4.46–4.41 (m, 1H, α-Ala), 4.00 (t, 2H, $J = 7.4$ Hz, NCH_2), 3.89–3.84 (m, 1H, α-Ala), 3.14–3.09 (m, 1H, β-Phe), 3.00–2.97 (m, 1H, β-Phe), 1.62–1.58 (m, 2H, NCH$_2$CH_2), 1.32 (d, 3H, $J = 7.0$ Hz, β-Ala), 1.31–1.28 (m, 6H, NCH$_2$CH$_2$(CH_2)$_3$CH$_3$), 1.25 (d, 3H, $J = 7.0$ Hz, β-Ala), 0.86 (t, 3H, $J = 6.8$ Hz, N(CH$_2$)$_5$CH_3).

*6.3.8. Synthesis of 6-{N′-[1-benzo[1,3]dioxol-5-yl-methylidene]hydrazino}-2-hexyl-benzo[de]isoquinoline-1,3-dione (**12**)*

Mixture of **1** (0.1 g, 0.32 mmol) and piperonal (0.05 g, 0.33 mmol) in 4.5 ml ethanol was boiled for 10 min in the presence of catalytic amount of acetic acid. The solution was allowed to crystallize at room temperature. The precipitate was filtered, washed with ethanol and purified by column chromatography on silica gel using chloroform/hexane/isopropanol (2:1.5:0.1) as eluent. Yield 0.07 g (50%); m.p. 195–198 °C. ^{1}H NMR (DMSO-d_6) δ ppm: 11.38 (s, 1H, C*H*=N), 8.76 (d, 1H, $J = 8.4$ Hz, Ar), 8.46 (d, 1H, $J = 7.2$ Hz, Ar), 8.36 (s, 1H, N*H*N=), 8.34 (d, 1H, $J = 8.6$ Hz, Ar), 7.77 (t, 1H, $J = 7.8$ Hz, Ar), 7.72 (d, 1H, $J = 8.5$ Hz, Ar), 7.44 (s, 1H, Ph), 7.21 (d, 1H, $J = 8.0$ Hz, Ph), 7.01 (d, 1H, $J = 7.9$ Hz, Ph), 6.11 (s, 2H, OCH_2O), 4.00 (t, 2H, $J = 7.5$ Hz, NCH_2), 1.63–1.58 (m, 2H, NCH$_2$CH_2), 1.34–1.28 (m, 6H, NCH$_2$CH$_2$(CH_2)$_3$CH$_3$), 0.86 (t, 3H, $J = 6.8$ Hz, N(CH$_2$)$_5$CH_3); UV–vis (DMSO): λ_{max} 460 nm.

6.4. Tissue treatment and incubation solutions

Wistar rats and Balb/c mice of both sexes were decapitated under ether anesthesia. Pieces of different organs were removed and either immediately frozen in liquid nitrogen or fixed in 2% formaldehyde in cacodilate buffer, pH 7.0 for 24 h at 4 °C. The fixed samples were then washed for 48 h at 4 °C in modified Holt's solution (15% sucrose, 1% gummy arabic in distilled water) (five changes of the washing

solution) and frozen in liquid nitrogen. Sections (10 μm) were cut at −25 °C and mounted on non-precooled gelatinized glass slides. Before the enzyme reactions all the sections were covered by celloidin (1% celloidin in absolute ethanol/diethyl ether/acetone 3:3:4) for a minute at room temperature.

DPP IV activity was localized in non-fixed sections, incubated in a substrate solution, consisting of 0.5 mmol substrate (Gly-Pro–HHNI) and 0.5 mg/ml aromatic aldehyde in 0.1 M phosphate buffer, pH 7.8 for 30–60 min at 37 °C.

TPP I activity was visualized in formaldehyde-fixed sections, incubated in substrate solution, consisting of 0.5 mmol substrate (Gly-Pro-Met–HHNI or Ala-Ala-Phe–HHNI) and 0.5 mg/ml aromatic aldehyde in 0.1 M acetate buffer, pH 4.5 for 3–6 h at 37 °C.

After the incubation all the sections were post-fixed in 4% neutral formalin for 15 min at room temperature, stained with haematoxyline consistent with classical methods of histology and embedded in glycerol/jelly.

6.5. Histochemical controls

To ensure that the localization of the histochemical reaction product specifically resulted from DPP IV or TPP I-catalyzed cleavage of the respective substrate, the following controls were done.

6.5.1. DPPIV

Control sections were pre-incubated in 0.5 mM solution of the inhibitor (Phe-Pro–NHONb) in 0.1 M phosphate buffer, pH 7.8 for an hour at room temperature. After that, the sections were moved to full substrate medium, supplied with 0.5 mM inhibitor and incubated for 60 min at 37 °C. Afterwards they were treated as above.

6.5.2. TPPI

Control sections were incubated in 0.01 mM inhibitor (Ala-Ala-Phe–chloromethyl ketone) in 0.1 M acetate buffer, pH 4.5 for an hour at room temperature. Then, they were transferred in full substrate medium, containing 0.01 mM inhibitor. After 3 h of incubation at 37 °C, the sections were treated as described above.

All the preparations were studied by light microscopy and fluorescent microscopy.

Acknowledgments

This work is supported by the Bulgarian Ministry of Education and Science, National Science Fund, Grant No. 1527/05.

Appendix. Supplementary data

Supplementary data associated with this article can be found in the online version at, doi: 10.1016/j.ejmech.2008.02.036.

References

[1] R. Gossrau, Histochemistry 60 (1979) 231–248.
[2] R. Mentlein, Regul. Pept. 85 (1999) 9–24.
[3] F. Bermpohl, K. Loster, W. Reutter, O. Baum, FEBS Lett. 428 (1998) 152–156.
[4] E. Boonacker, C.J.F. Van Noorden, Eur. J. Cell Biol. 83 (2003) 53–73.
[5] C. Antczak, I. De Meester, B. Bauvois, J. Biol. Regul. Homeost. Agents 15 (2001) 130–139.
[6] A.-M. Lambeir, C. Duriux, S. Scharpe, I. De Meester, Crit. Rev. Clin. Lab. Sci. 40 (2003) 209–294.
[7] Y. Aratake, T. Kotani, K. Tamura, Y. Araki, T. Kuribayashi, K. Konoe, S. Ohtaki, Am. J. Clin. Pathol. 96 (1991) 306–310.
[8] Y. Aratake, K. Umeki, K. Kiyoyama, Y. Hinoura, S. Sato, A. Ohno, T. Kuribayashi, K. Hirai, K. Nabeshima, T. Kotani, Diagn. Cytopathol. 26 (2002) 366–372.
[9] Y. Tlan, I. Sohar, J. Taylor, P. Lobel, J. Biol. Chem. 281 (2006) 6559–6572.
[10] D. Vines, M.J. Warburton, Biochim. Biophys. Acta 1384 (1998) 233–242.
[11] A.E. Page, K. Fuller, T.J. Chambers, M.J. Warburton, Arch. Biochem. Biophys. 306 (1993) 354–359.
[12] M.A. Junaid, G.M. Clark, R.K. Pullarkat, Int. J. Biol. Markers 15 (2000) 129–134.
[13] P.G. Du, S. Kato, Y.H. Li, T. Maeda, T. Yamane, S. Yamamoto, M. Fujiwara, Y. Yamamoto, K. Nishi, I. Ohkubo, Biol. Chem. 382 (2001) 1715–1725.
[14] K.E. Wisniewski, E. Kida, F. Cobnell, N. Zhong, Neurol. Sci. 21 (2000) 49–56.
[15] D.E. Sleat, R.M. Gin, I. Sohar, K. Wisniewski, S. Sklower-Brooks, R.K. Pullarkat, D.N. Palmer, T.J. Lemer, R.-M. Boustany, P. Uldall, A.N. Siakotos, R.J. Donnelly, P. Lobel, Am. J. Hum. Genet. 64 (1999) 1511–1523.
[16] S.E. Mole, R.-E. Williams, H.H. Goebel, Neurogenetics 6 (2005) 107–126.
[17] Y. Yayoi, Y. Ohsawa, M. Koike, G. Zhang, E. Kominami, Y. Uchiyama, Arch. Histol. Cytol. 64 (2001) 89–97.
[18] M. Koike, M. Shibata, Y. Ohsawa, S. Kametaka, S. Waguri, E. Kominami, Y. Uchiyama, Arch. Histol. Cytol. 65 (2002) 219–232.
[19] A. Dikov, M. Dimitrova, R. Krieg, K.-J. Halbhuber, Cell. Mol. Biol. 50 (2004) 553–558.
[20] A. Dikov, M. Dimitrova, R. Krieg, K.-J. Halbhuber, Cell. Mol. Biol. 50 (2004) 565–568.
[21] M.K. Kim, Q. Mao, B.L. Davidson, D.F. Wiemer, J. Med. Chem. 46 (2003) 1603–1608.
[22] B.L. Davidson, D. Wiemer, US Patent 6,824,998, B2 (2004).
[23] J. Gan, H. Tian, Q. Wang, K. Chen, in: Z.H. Kafafi (Ed.), Proceedings of SPIE, Organic Light-Emitting Materials and Devices V, vol. 4464, 2002, pp. 359–365.
[24] J. Gan, H. Tian, Z. Wang, K. Chen, J. Hill, P.A. Lane, M.D. Rahn, A.M. Fox, D.D.C. Bradley, J. Org. Chem. 645 (2002) 168–175.
[25] R. Thoma, B. Loeffler, M. Stihle, W. Huber, A. Ruf, M. Hennig, Structure 11 (2003) 947–959.
[26] S.L. Mayo, B.D. Olafson, W.A. Goddard III, J. Phys. Chem. 94 (1990) 8897–8909.
[27] W. Zhu, N. Minami, S. Kazaoui, Y. Kim, J. Mater. Chem. 14 (2004) 1924–1926.
[28] H.U. Demuth, R. Baumgrass, C. Schaper, G. Fischer, A. Barth, J. Enzym. Inhib. 2 (1988) 129–142.
[29] S.-C. Chang, R.E. Utecht, D.E. Lewis, Dyes Pigments 43 (1999) 83–94.